IEEE Photonics Journal
An IEEE Photonics Society Publication

Open Access

Ultralow Propagation Loss Slot-Waveguide in High Absorption Active Material

Volume 6, Number 3, June 2014

Yongzhuo Li
Kaiyu Cui
Xue Feng
Yidong Huang
Fang Liu
Wei Zhang

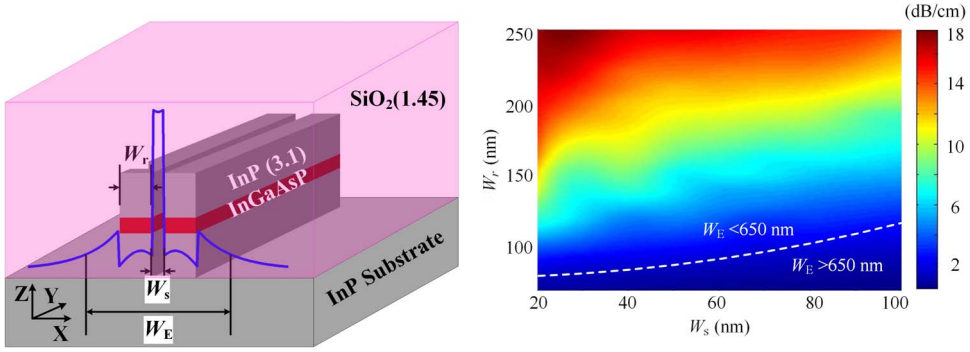

DOI: 10.1109/JPHOT.2014.2320746
1943-0655 © 2014 IEEE

IEEE photonics SOCIETY

IEEE

Ultralow Propagation Loss Slot-Waveguide in High Absorption Active Material

Yongzhuo Li, Kaiyu Cui, Xue Feng, Yidong Huang, Fang Liu, and Wei Zhang

Department of Electronic Engineering, Tsinghua National Laboratory for Information Science and Technology, Tsinghua University, Beijing 100084, China

DOI: 10.1109/JPHOT.2014.2320746

Manuscript received February 27, 2014; revised April 17, 2014; accepted April 19, 2014. Date of publication April 28, 2014; date of current version May 6, 2014. This work was supported in part by the National Basic Research Program of China under Grants 2011CBA00608, 2011CBA00303, and 2011CB301803 and in part by the National Natural Science Foundation of China under Grants 61307068, 61036011, and 61036010. Corresponding author: K. Cui (e-mail: kaiyucui@tsinghua.edu.cn).

Abstract: A slot waveguide formed by high absorption active material is proposed to reduce the propagation loss for monolithic integration. The low propagation loss is attained by concentrating the optical field inside the low-index slot region without absorption. The simulation results show that the propagation loss at 1.55 μm for the slot waveguide can be as low as 1.5 dB/cm in active material with an absorption coefficient of 3000 cm^{-1}, whereas the optical profile is set to be confined within 650 nm.

Index Terms: Waveguides, nanostructures, semiconductor materials.

1. Introduction

Photonic integrated circuits (PICs), consisted of active and passive devices linked by waveguides, have been developed for reducing cost and power consumption in the optical communications and signal processing systems [1]–[6]. For III–V compound semiconductor based monolithic integration, severe large propagation loss of the waveguide formed by using the same material as the active devices is unavoidable, because they have the same band gap for optical transition. It's reported that the propagation loss of the strip waveguides in the same material as the optical sources is very high and obviously unsuitable for monolithic integration [7]. Till now, there are two common solutions for this problem. One is to hybrid integrate the III–V compound semiconductors on silicon on insulator (SOI) substrates through bonding technology [8], [9]. The other approach is to remove the active layer and fabricate the waveguides using a regrowth technique [10]. Nevertheless, both solutions increase the difficulty of fabrication especially taking the alignment problem between nano-structures into account. Therefore, if a low loss waveguide could be achieved based on the same material of optical sources, the fabrication process will be greatly simplified, which is significant for the monolithic integration based on the same material, no matter for the silicon based or III–V compound based PIC.

Unlike the strip waveguide concentrated light inside the high-absorption core regions, the slot waveguide, which consists of a thin low-index slot embedded between high-index regions, can confine and guide light in low-index slot region with only nanometer scale, due to the large discontinuities at high index-contrast interfaces [11], [12]. Thus, the slot waveguide can effectively avoid the strong absorption in the high-index region. It has been reported that the propagation loss of Si slot waveguide can be as low as 5 dB/cm at optical wavelength of 1050 nm [13], which is

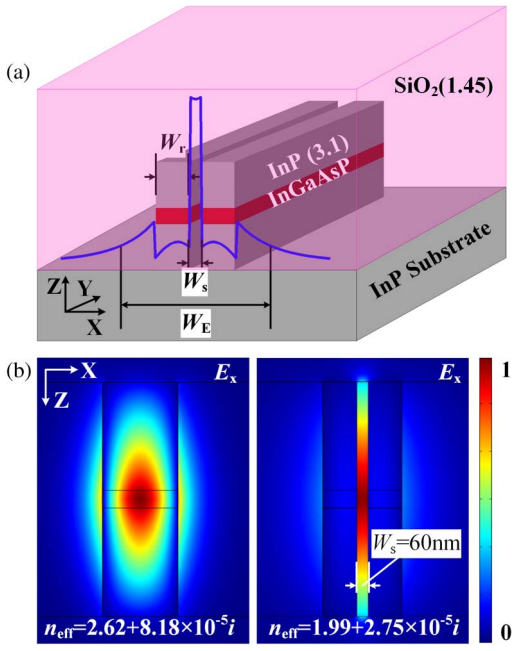

Fig. 1. (a) 3D schematic of the proposed slot waveguide in InP/InGaAsP/InP heterostructures and normalized transverse E-field (E_x) distribution of the fundamental TE eigenmode for the slot waveguide along the X axis; (b) The 2D fundamental modal field patterns (E_x component) of the strip and slot waveguides for TE polarization at wavelength $\lambda = 1.55$ μm.

closed to the propagation loss of $\sim$2 dB/cm for the slot waveguide at 1550 nm [14], [15]. However, the emission efficiency for III–V compound semiconductor is much higher than Si emitter at the state of art so that the power consumption of a monolithic PIC based on group III–V material maybe much lower. Therefore, a slot waveguide based on commonly used InP/InGaAsP/InP hetero-structures for telecom-wavelength, which contains quantum wells, is simulated and optimized to reduce the propagation loss for monolithic integration. Simulated results show that the propagation loss could be as low as 1.5 dB/cm based on InP/InGaAsP/InP heterostructures with absorption coefficient of 3000 cm^{-1} for the InGaAsP active core layer [16]. Therefore, the slot waveguide provides a potential propagation solution for monolithic integration based on the same material.

2. Structure of the Slot Waveguide

The schematic of the slot waveguide is shown in Fig. 1(a), which consists of a thin slot sandwiched between two high-index regions. The width of slot and high-index regions are noted as W_s and W_r, respectively. The high-index region is vertically formed by two 600-nm-thick InP cladding layers (gray regions, refractive index $n_c = 3.1$) and an embedded 100-nm-thick InGaAsP active core layer (red region). In this paper, slot waveguides are designed in the InP/InGaAsP/InP heterostructures, which are typical candidates for telecom-wavelength lasers or LEDs. For the InP/InGaAsP/InP heterostructures, the core material has higher absorption/gain coefficient than cladding material, and the optical field is confined in the core layer with high absorption/gain coefficient due to the refractive index difference between InP and InGaAsP. The absorption of the InP cladding layer for light at 1550 nm is very low. While the absorption coefficient of the InGaAsP active core layer is as high as 3000 cm^{-1}, which is evaluated from the quantum wells structure included in this layer [16]. The detailed parameter of the quantum wells is listed in Table 1. Due to the weak refractive index between InP and InGaAsP, the optical mode is extended over 1 μm in the vertical direction. So the thickness of InP layer is chosen to be 600 nm. Different to Si slot waveguide, in our proposed structure, only a small fraction of optical field is overlapped with the active layer (InGaAsP quantum wells) due to the weak refractive index distribution in the vertical direction. Around the slot

TABLE 1

Detailed parameter of the quantum wells

Item name	Material component	Thickness
Quantum well (5 layers)	$In_{0.73}Ga_{0.27}As_{0.85}P_{0.15}$	5.5 nm
Barrier (6 layers)	$In_{0.75}Ga_{0.25}As_{0.54}P_{0.45}$	10 nm

waveguide silicon dioxide is considered as cladding (pink region, refractive index $n_s = 1.45$), which is easy to fabricated by spinning SOG (Spin on Glass). Also, it can be coated by polymer with low refractive index and low absorption efficient at 1550 nm [17], or even void for some sensing applications [18].

Since the slot waveguide enables the optical field to be concentrated inside the low-index slot regions without material absorption, as indicated in the blue line of Fig. 1(a), low propagation loss of slot waveguide could be predicted even within strong absorption active material. For qualitative research, the optical modes of slot waveguides are numerically simulated based on the finite element method (FEM) combining with a complex refractive index. Then the propagation loss can be obtained from the imaginary part of the effective refractive index (n_{eff}) of the guided mode, as shown in

$$\alpha = 20k_0 In_{\text{eff},i} \lg e \quad (\text{dB}) \tag{1}$$

where, k_0 is the wavevector in the air, $n_{\text{eff,i}}$ is the imaginary part of the guided-mode's effective refractive index, l is the length of the slot waveguide. Here, effective complex refractive index of $n_a = 3.4 + 3.74 \times 10^{-4} i$, corresponding to a high absorption coefficient of 3000 cm^{-1} [16], is adopted to character the absorption of the active media.

The optical modes of a slot waveguide and a strip waveguide calculated by FEM with the referred complex refractive index are compared and shown in Fig. 1(b), which are the respective fundamental modal field patterns of E_x component for TE polarization at wavelength $\lambda = 1.55$ μm. It can be seen that, in the strip waveguides, the vast majority of optical field is overlapped with the high index region. While, in the slot waveguides, a large fraction of optical field is confined in low-index slot region. Also, due to the difference of mode profile, the effective refractive index of such two waveguides are quite different ($2.62 + 8.18 \times 10^{-5} i$ vs $1.99 + 2.75 \times 10^{-5} i$). From the imaginary part of the propagation constant of the two guided modes, the propagation loss of the strip waveguide with width of 420 nm is 28.5 dB/cm, while that of the slot waveguide with total width of 420 nm ($W_s = 60$ nm and $W_r = 180$ nm) is only 9.5 dB/cm. These results demonstrate that the slot waveguide can effectively reduce propagation loss even using a material with high absorption coefficient, since a large portion of the optical field is concentrated inside the low-index slot region.

3. Optimization of the Slot Waveguide

As the proportion of the optical field inside the slot region can be controlled by the proposed structure, the dependence of propagation loss on the slot width and high-index regions' width is investigated. To give the overall propagation losses under various widths of slot and high-index regions, the calculated results are summarized in Fig. 2, where W_s ranges from 20 to 100 nm and W_r spans from 70 to 250 nm. It should be noted that when $W_s > 100$ nm and $W_r < 70$ nm, the slot waveguide cannot support any guided mode. As indicated in Fig. 2, narrow high-index regions and a wide slot are favourable for reducing propagation losses of slot waveguides. The lowest propagation loss is 0.4 dB/cm at $W_s = 100$ nm and $W_r = 70$ nm. But the electric field will spread with narrow high-index regions and a wide slot. The dashed white line in Fig. 2 indicates the width of electric field, $W_E = 650$ nm, which equals the width of electric field for 500-nm-wide silicon

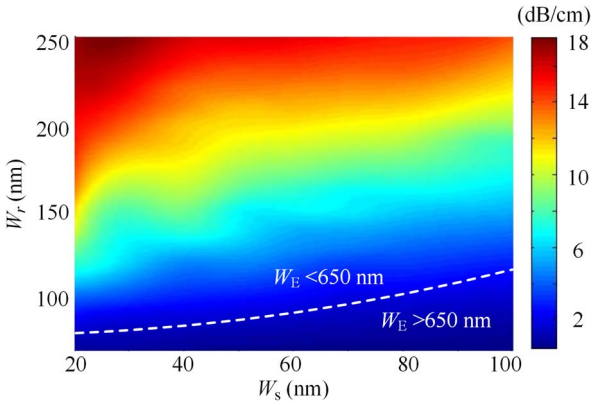

Fig. 2. Simulation results for the propagation losses of slot waveguides with w_r ranging from 70 to 250 nm and w_s ranging from 20 to 100 nm.

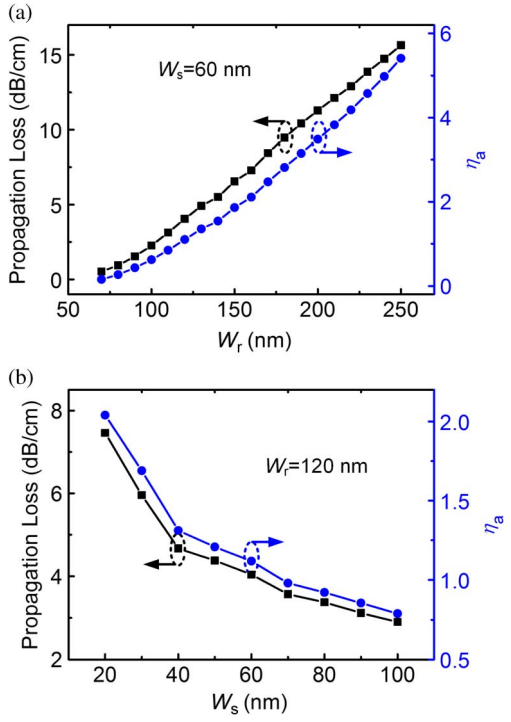

Fig. 3. (a) Propagation losses and η_a for the slot waveguides under different W_r with a fixed slot width $W_s = 60$ nm. (b) Propagation losses and for the slot waveguides under different W_s with a fixed width of high-index region $W_r = 120$ nm.

waveguide surrounded by silicon dioxide. Above the white line, W_E is less than 650 nm, while below that, W_E is larger than 650 nm. Then if we optimize the slot waveguide under the condition of $W_E < 650$ nm, the lowest propagation loss is 1.5 dB/cm at $W_s = 60$ nm and $W_r = 90$ nm, which is close to the well fabricated silicon waveguide at 1.55 μm [19].

The reasons for the dependence of the propagation loss on the slot structure can be explained by the optical mode ($|E_x|^2$) in the active core layer as a percentage of that in the total regions (named as η_a), which is summarized in Fig. 3. With the slot width fixed at 60 nm, the propagation losses of slot waveguides are calculated under the width of high-index regions in range of 70-250 nm, and the results are summarized in Fig. 3(a) (black line). To reduce the width of each high-index region from 250 to 70 nm leads to a monotonic decrease in propagation loss from 15.6 to 0.5 dB/cm. Because

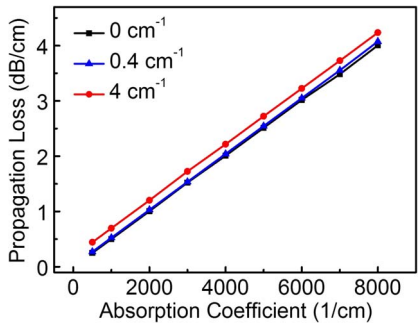

Fig. 4. The propagation losses under different absorption coefficients of the active core layer and cladding (SiO_2).

η_a declines from 5.4% to 0.16% with the decreasing width of high-index region, as shown in the blue line of Fig. 3(a). On the other hand, when the width of high-index regions is set as $W_r = 120$ nm, the propagation losses and η_a are calculated with W_s in the range of 20 to 100 nm, as shown in Fig. 3(b). Notice that the propagation losses gradually decrease from 7.5 to 2.9 dB/cm with increased W_s due to η_a decreasing from 2% to 0.8%. Therefore, narrow high-index regions and a wide slot can reduce η_a and further reduce propagation losses for slot waveguides.

Finally, the propagation losses under different absorption coefficients of the active core layer and cladding (SiO_2) are calculated for more realistic applications with the optimized structure parameter as aforementioned. The absorption coefficients of SiO_2 are set between 0 to 4 cm^{-1} [20]. As shown in Fig. 4, the calculation results show that the propagation losses are only increased about 0.2 dB/cm with the absorption coefficients of SiO_2 increased from 0 to 4 cm^{-1}. Therefore, the influence of absorption from SiO_2 on the propagation losses is limited. What's more, the propagation loss has a basically linear relation with the absorption coefficient of the active core layer. Compared with the propagation loss of 42 dB/cm for the strip waveguide based on InP/InGaAsP/InP [5], the propagation loss of slot waveguide, coated by SiO_2 with absorption efficient of 4 cm^{-1}, is only in range of 0.4–4.2 dB/cm with the absorption coefficient of active core layer between 500 cm^{-1} and 8000 cm^{-1}. This promising result indicates that adopting slot waveguide is a potential solution for monolithic integration based on the same active III–V material. In addition, the lossless coupling structures between slot waveguide and strip waveguide have also been demonstrated [21]–[23], which allows the compatibility of slot structure waveguides with other devices. Moreover, the feasibility of fabricating slot waveguide based on InP/InGaAsP/InP heterostructures has been verified in our previous work [24]. The etching depth of 40-nm-width slot could be more than 1.8 μm by inductively coupled plasma (ICP) etching, which corresponds to a record-high aspect-ratio of 45.

4. Conclusion

In conclusion, utilizing a slot waveguide based on the same active material with optical sources is proposed and studied to reduce the propagation loss for monolithic integration. The propagation loss of a slot waveguide is calculated based on a practical example formed by III–V compound material with an absorption coefficient of 3000 cm^{-1}. Given the limitation of width of electric field, widths of slot and high-index regions are optimized to reach the lowest propagation loss of 1.5 dB/cm for the slot waveguide at 1.55 μm with the entire structure covered by silicon dioxide. Based on the optimized structure parameter, the simulated propagation loss less than 4.2 dB/cm is obtained under different absorption coefficients in range of 500 to 8000 cm^{-1}. It should be noted that the slot structure can also be extended to other structures, such as horizontal slot waveguide or slot photonic crystal waveguide for realizing ultralow propagation loss in high absorption active material. Therefore, the slot waveguide provides a potential solution for monolithic integration based on the same material.

References

[1] F. A. Kish *et al.,* "Current status of large-scale inp photonic integrated circuits," *IEEE J. Sel. Topics Quantum Electron.*, vol. 17, no. 6, pp. 1470–1489, Nov./Dec. 2011.
[2] H. T. Hattori *et al.,* "Heterogeneous integration of microdisk lasers on silicon strip waveguides for optical interconnects," *IEEE Photon. Technol. Lett.*, vol. 18, no. 1, pp. 223–225, Jan. 2006.
[3] Y. Halioua *et al.,* "Hybrid III-V semiconductor/silicon nanolaser," *Opt. Exp.*, vol. 19, no. 10, pp. 9221–9231, May 2011.
[4] D. Liang *et al.,* "High-quality 150 mm InP-to-silicon epitaxial transfer for silicon photonic integrated circuits," *Electrochem. Solid-State Lett.*, vol. 12, no. 1, pp. H101–H104, Jan. 2009.
[5] A. Himeno, K. Kato, and T. Miya, "Silica-based planar lightwave circuits," *IEEE J. Sel. Topics Quantum Electron.*, vol. 4, no. 6, pp. 913–924, Nov./Dec. 1998.
[6] X. Zhang, A. Hosseini, X. Lin, H. Subbaraman, and R. T. Chen, "Polymer-based hybrid-integrated photonic devices for silicon on-chip modulation and board-level optical interconnects," *IEEE J. Sel. Topics Quantum Electron.*, vol. 19, no. 6, pp. 196–210, Nov./Dec. 2013.
[7] S. Dupont *et al.,* "Low-loss InGaAsP/InP submicron optical waveguides fabricated by ICP etching," *Electron. Lett.*, vol. 40, no. 14, pp. 865–866, Jul. 2004.
[8] J. Hofrichter *et al.,* "A single InP-on-SOI microdisk for high-speed half-duplex on-chip optical links," *Opt. Exp.*, vol. 20, no. 26, pp. B365–B370, Dec. 2012.
[9] M. Heck *et al.,* "Hybrid silicon photonics for optical interconnects," *IEEE J. Sel. Topics Quantum Electron.*, vol. 17, no. 2, pp. 333–346, Mar./Apr. 2011.
[10] K. Nozaki, H. Watanabe, and T. Baba, "Photonic crystal nanolaser monolithically integrated with passive waveguide for effective light extraction," *Appl. Phys. Lett.*, vol. 92, no. 2, pp. 021108-1–021108-3, Jan. 2008.
[11] Q. F. Xu, V. R. Almeida, R. R. Panepucci, and M. Lipson, "Experimental demonstration of guiding and confining light in nanometer-size low-refractive-index material," *Opt. Lett.*, vol. 29, no. 14, pp. 1626–1628, Jul. 2004.
[12] V. R. Almeida, Q. F. Xu, C. A. Barrios, and M. Lipson, "Guiding and confining light in void nanostructure," *Opt. Lett.*, vol. 29, no. 11, pp. 1209–1211, Jun. 2004.
[13] H. Morino, T. Maruyama, and K. Iiyama, "Propagation of lossy wave in Si Slot waveguide," in *Proc. IEEE Int. Conf. Group IV Photon. GFP*, 2012, pp. 228–230ThE1.
[14] A. Spott *et al.,* "Photolithographically fabricated low-loss asymmetric silicon slot waveguides," *Opt. Exp.*, vol. 19, no. 11, pp. 10 950–10 958, May 2011.
[15] R. Ding *et al.,* "Low-loss asymmetric strip-loaded slot waveguides in silicon-on-insulator," *Appl. Phys. Lett.*, vol. 98, no. 3, pp. 233303-1–233303-3, Jun. 2011.
[16] L. A. Coldren and S. W. Corzine, *Diode Lasers and Photonic Integrated Circuits*. New York, NY, USA: Wiley, 1995.
[17] X. Zhang *et al.,* "Wide optical spectrum range, subvolt, compact modulator based on an electro-optic polymer refilled silicon slot photonic crystal waveguide," *Opt. Lett.*, vol. 38, no. 22, pp. 4931–4394, Nov. 2013.
[18] N. A. C. Manaf, M. H. M. Yusoff, and M. K. Abd-Rahman, "Optimized nano-slot silicon waveguide structures for optical sensing applications," *Adv. Mater. Res.*, vol. 832, pp. 212–217, 2013.
[19] J. Cardenas *et al.,* "Low loss etchless silicon photonic waveguides," *Opt. Exp.*, vol. 17, no. 6, pp. 4752–4757, Mar. 2009.
[20] R. Kitamura, L. Pilon, and M. Jonasz, "Optical constants of silica glass from extreme ultraviolet to far infrared at near room temperature," *Appl. Opt.*, vol. 46, no. 33, pp. 8118–8133, Nov. 2007.
[21] Z. C. Wang *et al.,* "Ultracompact low-loss coupler between strip and slot waveguides," *Opt. Lett.*, vol. 34, no. 10, pp. 1498–1500, May 2009.
[22] N. N. Feng, R. Sun, L. C. Kimerling, and J. Michel, "Lossless strip-to-slot waveguide transformer," *Opt. Lett.*, vol. 32, no. 10, pp. 1250–1252, May 2007.
[23] R. Palmer *et al.,* "Low-loss silicon strip-to-slot mode converters," *IEEE Photon. J.*, vol. 5, no. 1, p. 2200409, Feb. 2013.
[24] K. Cui, Y. Li, X. Feng, Y. Huang, and W. Zhang, "Fabrication of high-aspect-ratio double-slot photonic crystal waveguide in InP heterostructure by inductively coupled plasma etching using ultra-low pressure," *AIP Adv.*, vol. 3, no. 2, p. 022122, Feb. 2013.